JOURNAL OF OPTOELECTRONICS AND ADVANCED MATERIALS, Vol. 10, No. 9, September 2008, p. 2466 - 2469

Synthesis of nanocrystalline zinc sulphide and preparation of its self-assembled thin films

JASIM M. ABBAS, CHARITA MEHTA, G. S. S. SAINI, S. K. TRIPATHI*
Department of Physics, Centre of Advanced Study in Physics, Panjab University, Chandigarh – 160 014, India

We have synthesized ZnS nano-crystalline (n-ZnS) powder using zinc acetate and thiourea from chemical route at different pH. The average crystal size is determined as 3-5 nm with the help of X-ray diffraction. The formation of ZnS has been confirmed with the help of infrared (IR) spectroscopy by observing bands corresponding to the multi phonon absorption. IR spectrum also confirms presence of the capping agent on ZnS. Thin films of ZnS have also been deposited on glass and quartz substrates from the solution using self-aggregation approach. Refractive index (n) of the films is also determined. The optical band gap is calculated from the Tauc's extrapolation and is found to be dependent on pH of the bath solution. Electrical conductivity measurements have been done on these thin films and the activation energy has been calculated.

(Received April 28, 2008; accepted August 14, 2008)

Keywords: n-ZnS, Self-assembling, Optical band gap, Electrical conductivity

1. Introduction

In recent years, properties of nanosized materials have generated a great deal of interest because of the science involved in these studies and technological applications of these materials. As the physical dimensions of the particle approach to the nanometer scales, quantization and surface effects begin to play an important role, leading to drastic changes in the measured properties [1]. Semiconductor nanoparticles have attracted much attention because of their novel electric and optical properties originating from surface and quantum confinement effects [2-5]. ZnS is a II-VI semi conducting material with a wide direct band gap of 3.65 eV in the bulk. It has potential applications in optoelectronic devices such as blue light emitting diodes [6], electroluminescence devices and photovoltaic cells which enable wide applications in the field of displays [7-8], sensors and lasers [9]. In recent years, nanocrystalline ZnS attracted much attention because the properties in nanoforms differ significantly from those of their bulk counterparts. Therefore, much effort has been made to control the size, morphology and polycrystallinity of the ZnS nanocrystals with a view to tune their physical properties. Hence, there has been growing interest in developing techniques for preparing semiconductor nanoparticles and films. The wet chemical synthesis method is a simple and inexpensive alternative to more complex chemical vapor deposition (CVD) and physical techniques. The physical methods [10], which are commonly used for the fabrication of nanomaterials, have some resolution limits that restrict these techniques from reaching the nanometer scale. On the other hand, the wet chemical technique offers a simple means to synthesize such particle with good control of size and size distribution [11]. Therefore, the authors have decided tp prepare the n-ZnS powder and thin films with varying deposition parameter such as pH of the bath solution. Section 2 describes the experimental details. The results have been presented and discussed in section 3. The last section deals with the conclusion of this work.

2. Experimental

We have synthesized ZnS nano-crystalline powder from chemical route at different pH (= 7, 10,12) with capping agent (tri-sodium citrate). Aqueous solution of ZnS has been prepared by dissolving a nominal amount of zinc-acetate, capping agent (tri-sodium citrate) and thiourea for sulfide ion source in 50 ml deionized water and the resultant mixture has been stirred at elevated temperature. The solid phase is isolated by filtration and finally dried in hot bath, from the residue solution. This solid phase consists of ZnS nano-crystals. Thin films have been deposited on cleaned glass, quartz substrates and KBr pallets for the optical, electrical and structural measurements.

Crystallographic study has been carried out using a Phillips PW-1610 X-ray diffractometer using CuK_α radiation in the 2θ range from 10° to 70°. The IR spectrum is determined on a Perkin-Elmer PE-Rx 1 FTIR spectrophotometer. The spectral resolution of the IR spectrophotometer was 1 cm^{-1} throughout the experiment. To study the optical properties of n-ZnS thin films, the transmission spectra are recorded using a double beam UV/VIS/NIR spectrometer [Hitachi-330] in the transmission range 300-1000 nm for all samples. The electrical measurements of these thin films were carried out in a specially designed metallic sample holder. A vacuum of about 10^{-3} mbar is maintained throughout these measurements. Planar geometry of the films (length ~ 1.0 cm; electrode gap ~ 8×10^{-2} cm) is used for the electrical

measurements. Thick In electrodes were used for the electrical contacts. Thickness of the film is measured as ~ 615 nm with a profile meter. The electrical conductivity is noted manually from a digital picoammeter (DPM-11 Model). The accuracy in current measurements is typically 1 pA.

3. Results and discussion

Fig. 1 shows the XRD pattern of n-ZnS film deposited on the glass substrates (pH = 12). The spectrum in figure 1 shows the diffraction peaks at 2θ values of 29.5°, 48.7° and 57.5° on the film deposited at pH = 12. The highest intensity reflection peak is at 2θ = 29.5° [111], with two

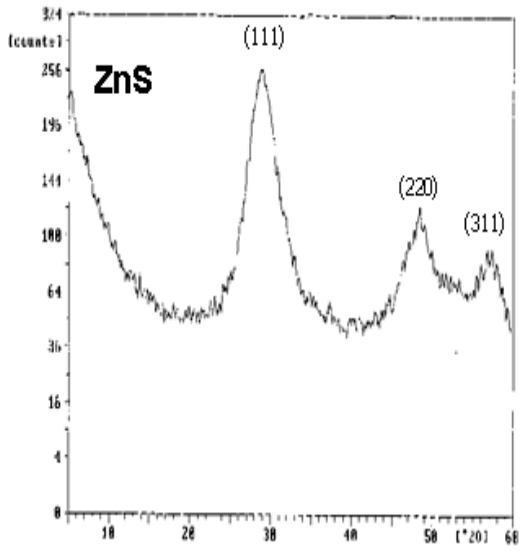

Fig. 1. XRD plot of n-ZnS at pH = 12.

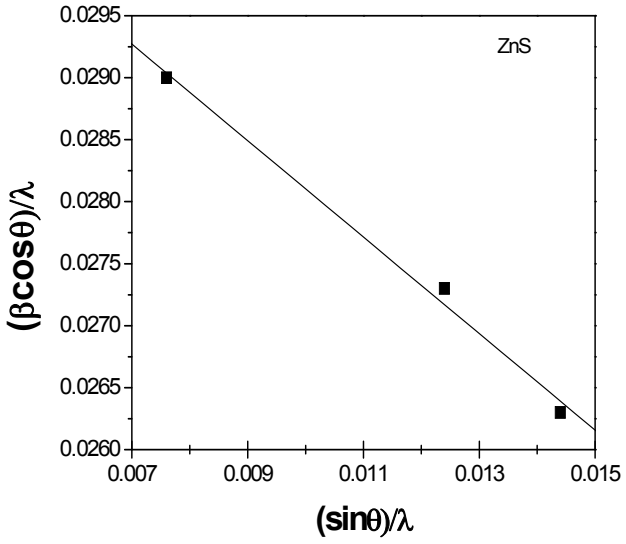

Fig. 2. Plot between ((βcosθ)/λ vs (sin θ)/λ for n-ZnS film at pH = 12.

another small intensity peaks at 2θ = 48.7° [220] and 57.5° [311] indicating that [111] is the preferred direction. The intensity of these peaks increases as the pH value decreases (results not shown here). The comparison of observed `d' values with standard `d' values [12,13] confirms the sphalerite cubic (zinc blende type) nanocrystalline structure of ZnS thin films.

Information of the strain and the particle size are obtained from the full width at half maximum (FWHMs) of the diffraction peaks. The FWHMs (β) can be expressed as a linear combination of the contributions from the strain (ε) and particle size (L) through the following relation [14]

$$\frac{\beta\cos\theta}{\lambda} = \frac{1}{L} + \frac{\varepsilon\sin\theta}{\lambda} \qquad (1)$$

Fig. 2 shows the plot of ($\beta\cos\theta$)/λ versus (sin θ)/λ for n-ZnS film at (pH = 12) which is a straight line. The reciprocal of intercept on the ($\beta\cos\theta$)/λ axis gives the average particle size as ~ 4 nm. The particle size increases (4.6 nm and 5.4 nm) as the pH value decreases from 12 to 10 and 7 respectively.

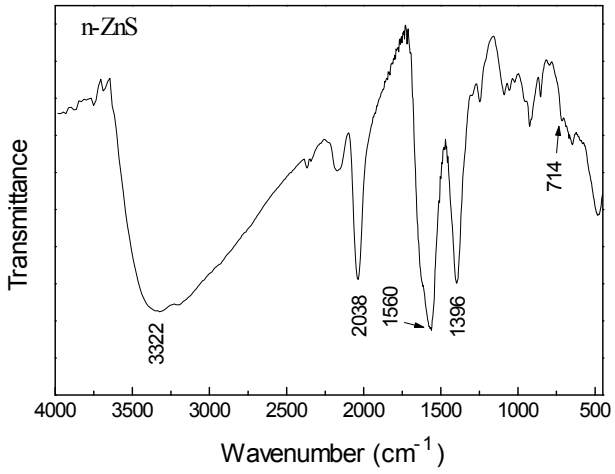

Fig. 3. IR spectrum of n-ZnS in wavenumber region 4000-450 cm^{-1}.

Fig. 3 shows the IR spectrum of n-ZnS film deposited at the KBr pallet. The presence of the band in the spectrum at 714 cm^{-1} confirms the formation of ZnS. Further bands at 1396 cm^{-1} and 1560 cm^{-1} confirms the presence of capping agent trisodiumcitrate used for above study. The former band can be assigned to symmetric stretching of COO^-, while the later band can be assigned to the asymmetric COO^- [15]. Another band at 3322 cm^{-1} can be assigned to OH stretching of trisodium citrate. The presence of the above mentioned bands indicate that trisodium citrate is bounded to the ZnS nanocrystals and it is arresting the growth of bulk crystals of ZnS.

Optical properties are studied by recording the transmission spectra of the films. Figure 4 shows the

transmission data of n-ZnS thin films deposited at different pH. The value of refractive index has been calculated using the relation [16]:

$$n = [\{2n_S (1-T)^{1/2} + n_S (2-T)\}/T]^{1/2} \quad (2)$$

Fig. 5 shows the plots of refractive index (n) vs hυ for all three thin films deposited at different pH values of the bath solution. It is clear from the figure that the value of n increases as the value of hυ increases. It is also clear from these plots that the value of n increases as the value of pH increases (as the particle size decreases). This increase in the value of n may be due to the quantum confinement effect due to the decrease in the particle size.

From the transmission data (see figure 4), nearly at the fundamental absorption edge, the values of absorption coefficient (α), are calculated in the region of strong absorption using the relation

$$\alpha = \frac{1}{d}\ln\left(\frac{1}{T}\right) \quad (3)$$

The fundamental absorption, which corresponds to the transition from valence band to conduction band, can be used to determine the band gap of the material. The relation between α and the incident photon energy ($h\nu$) can be written as [17]

$$\alpha = \frac{A\left(h\nu - E_g\right)^n}{h\nu} \quad (4)$$

where A is a constant, E_g is the band gap of the material and the exponent n depends on the type of transition. The n may have values 1/2, 2, 3/2 and 3 corresponding to the allowed direct, allowed indirect, forbidden direct and forbidden indirect transitions, respectively.

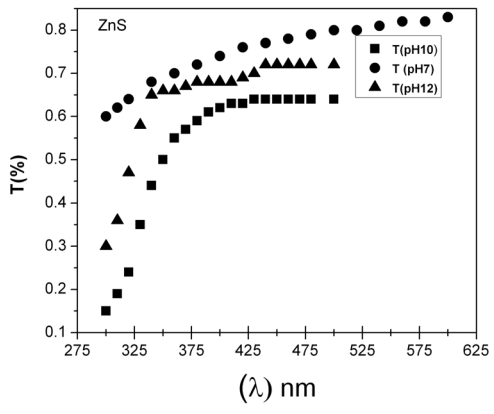

Fig. 4. Transmission curve of n-ZnS thin films.

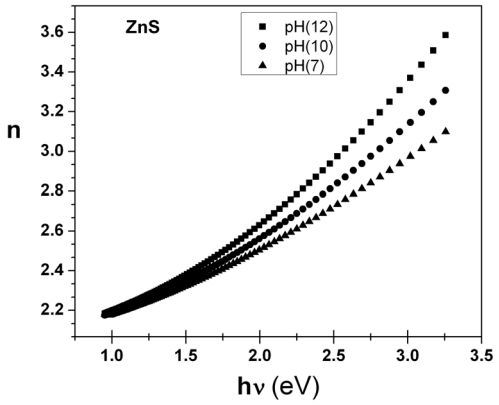

Fig. 5. Plots between n vs hυ.

The value of optical gap is calculated by extrapolating the straight line portion of $(\alpha h\nu)^{1/n}$ vs $h\nu$ graph to $h\nu$ axis taking $n = 0.5$. Fig. 6 shows the plots of $(\alpha h\nu)^2$ vs $h\nu$ for the films deposited at different pH values. The correct values of the optical gap calculated from the figure are (3.40 ± 0.01) eV, (3.68 ± 0.01) eV and (3.80 ± 0.01) eV for the films deposited at different pH i.e. 7, 10 and 12 respectively. The value of optical gap is found to decrease with the increase in the pH value. These values of optical gap are inserted in Table 1. Clearly, the observed values of E_g are higher than the value of bulk optical gap of n-ZnS [(3.3 ± 0.01) eV] [18] due to quantum confinement in the n-ZnS nanocrystallites.

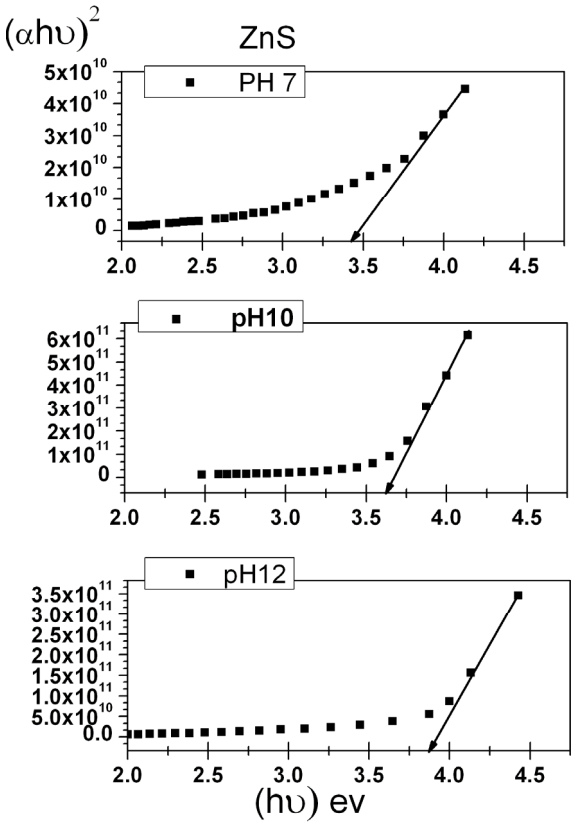

Fig. 6. Plots of $(\alpha h\upsilon)^2$ vs hυ at different pH.

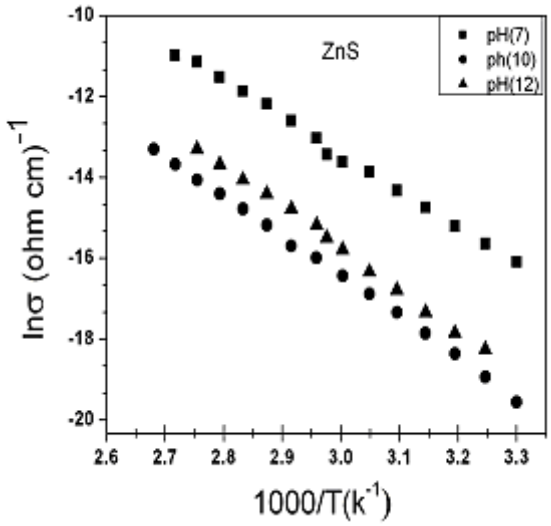

Fig. 7. Plots of ln σ_d vs 1000/T of n-ZnS thin films at different pH.

Table 1.The electrical and optical parameters of n-ZnS powder.

pH	E_g (eV) (± 0.01)	Particle size (nm)	σ_d ($\Omega^{-1}cm^{-1}$)	E_a (eV) (± 0.01)
12	3.80	4.0	(1.9 ± 0.02) $\times10^{-8}$	0.87
10	3.68	4.6	(1.6 ± 0.02) $\times10^{-7}$	0.80
7	3.40	5.4	(5.7 ± 0.02) $\times10^{-6}$	0.76

3.2 Electrical Properties

Fig. 7 shows the temperature dependence of dark conductivity (σ_d) of n-ZnS thin films deposited at different pH (12, 10 and 7). The electrical conductivity shows typical Arrhenius type of activation

$$\sigma_d = \sigma_o \exp\left(\frac{-\Delta E}{kT}\right) \quad (5)$$

where ΔE is the activation energy for dc conduction and k is the Boltzmann's constant. The values of σ_d, calculated using Eq. (6), are (1.9 ± 0.02)×10^{-8} $\Omega^{-1}cm^{-1}$, (1.6 ± 0.02)×10^{-7} $\Omega^{-1}cm^{-1}$ and (5.7 ± 0.02)×10^{-6} $\Omega^{-1}cm^{-1}$ for the films deposited at different pH values 12, 10 and 7 respectively. The value of σ_d increases as the particle size of n-ZnS increases. The increase in electrical conductivity and decrease in the activation energies as the value of pH decreases may be due to the change in structural parameters, improvement in crystallite and grain size, decrease in inter-crystallite boundaries (grain boundary domains) and removal of some impurities (adsorbed and absorbed gases).

4. Conclusions

n-ZnS powder as well as thin films have been deposited at different pH values of the deposition bath solution. These films have been deposited at different substrates. The particle size has been calculated using XRD data and found to be 4-6 nm. FTIR data confirm the formation of ZnS nanoparticles. The optical band gap has been calculated using optical data and it is found that the band gap increases as the pH value increases which is due to the quantum confinement effect. Electrical conductivity measurements have been done and it is found that the dark conductivity increases and dark activation energy decreases as the particle size increases.

Acknowledgements

This work is financially supported by DST (Major Research Project), New Delhi.

References

[1] A.P. Alivisatos, Science **271**, 933 (1996).
[2] G.Z. Wang, W. Chen, C.H. Liang, Y.W. Wang, G. W. Meng, L.D. Zhang, Inorg. Chem. Commun. **4**, 208 (2001).
[3] L.E. Brus, Appl. Phys. A **53**, 465 (1991).
[4] R. Maity, K.K. Chattopadhyay, Nanotechnology **15**, 812 (2004).
[5] S. Neeleshwar, C.L. Chen, C.B. Tsai, Y.Y. Chen, Phys. Rev. B **71**, 201307(R) (2005).
[6] S. Coe, W.K. Woo, M.G. Bawendi, V. Bulovic, Nature **420**, 800 (2002).
[7] M.C. Beard, G.M. Turner, C.A. Schmuttenmaer, Nano Lett. **2**, 983 (2002).
[8] R.P. Raffaelle, S..L. Castro, A.F. Hepp, S.G. Bailey, Prog. Photovoltaics **10**, 433 (2002).
[9] V.I. Klimov, A.A. Mikhailovsky, S. Xu, A. Malko, J.A. Hollingsworth, C.A. Leatherdale, H.J. Eisler, M.G. Bavendi, Science **290**, 314 (2000).
[10] A.P. Alivisatos, Mater. Res. Soc. Bull. **23**, 18 (1998).
[11] B. Zhang, J. Mu, D. Wang, J. Dispersion Sci. & Technol. **26**, 521 (2005).
[12] JCPDS Data File No. 8-459.
[13] JCPDS Data File No. 19-191.
[14] S.B. Qadri, E.F. Skelton, D. Hsu, A.D Dinsmore, J. Yang, H.F. Gray, B.R. Ratna, Phys. Rev. B **60**, 9191 (1999).
[15] X. Zou, E. Ying, S. Dong, Nanotechnology **17**, 4758 (2006).
[16] J.C. Manifacier, J. Gasiot, J.P. Fillard, Thin Solid Films **77**, 67 (1981).
[17] J.I. Pankove, Optical Processes in Semiconductors, Englewood Cliffs. NJ: Prentice-Hall (1971).
[18] X. Zhong, S. Liu, Z. Zhang, L. Li, Z. Wei, W. Knoll, J. Mater. Chem. **14**, 2790 (2004).

*Corresponding author: surya@pu.ac.in; gsssaini@pu.ac.in

JOURNAL OF OPTOELECTRONICS AND ADVANCED MATERIALS, Vol. 10, No. 9, September 2008, p. 2466 - 2469